

MIT Open Access Articles

Meshes Preserving Minimum Feature Size

The MIT Faculty has made this article openly available. **Please share** how this access benefits you. Your story matters.

Citation: Aloupis, Greg, Erik D. Demaine, Martin L. Demaine, Vida Dujmovic, and John Iacono. "Meshes Preserving Minimum Feature Size." *Lecture Notes in Computer Science* (2012): 258–273.

As Published: http://dx.doi.org/10.1007/978-3-642-34191-5_25

Publisher: Springer-Verlag

Persistent URL: <http://hdl.handle.net/1721.1/86202>

Version: Author's final manuscript: final author's manuscript post peer review, without publisher's formatting or copy editing

Terms of use: Creative Commons Attribution-Noncommercial-Share Alike



Meshes Preserving Minimum Feature Size

Greg Aloupis^{1*}, Erik D. Demaine², Martin L. Demaine²,
Vida Dujmović³, and John Iacono^{4**}

¹ Université Libre de Bruxelles. aloupis.greg@gmail.com

² Massachusetts Institute of Technology, Cambridge, Massachusetts, USA.
{edemaine,mdemaine}@mit.edu

³ Carleton University, Ottawa, Ontario, Canada. vida@cs.mcgill.ca

⁴ Polytechnic Institute of New York University, Brooklyn, New York, USA. jiacono@poly.edu

Abstract. The *minimum feature size* of a planar straight-line graph is the minimum distance between a vertex and a nonincident edge. When such a graph is partitioned into a mesh, the *degradation* is the ratio of original to final minimum feature size. For an n -vertex input, we give a triangulation (meshing) algorithm that limits degradation to only a constant factor, as long as Steiner points are allowed on the sides of triangles. If such Steiner points are not allowed, our algorithm realizes $O(\lg n)$ degradation. This addresses a 14-year-old open problem by Bern, Dobkin, and Eppstein.

1 Introduction

Meshing is a field frequently studied in the context of computational geometry; see [BE95,She04] for surveys. In two dimensions, the typical forms of input are point sets, polygons, and most generally, planar straight-line graphs (PSLGs). The typical desired output is a decomposition into triangles or quadrangles, usually with Steiner points allowed (though usually aiming to minimize their number). A wide variety of quality measures dictate the desired decomposition. Often, decompositions are constructed so that there are no large angles, or instead no small angles, short edges, or short triangle heights. Most of these problems have been solved in the best sense possible. This paper highlights one problem that has not been fully solved.

Problem statement. Our goal is to mesh a polygon P into a triangulation G while avoiding the introduction of a small (Euclidean) distance between a vertex and a nonincident edge in G , compared to distances already existing in P . The minimum such distance in G (or more generally in any PSLG) is called the *minimum feature size*, denoted by $\text{mfs}(G)$. See [Rup93,Dey07,HMP06,Eri03]. We call the ratio $\frac{\text{mfs}(P)}{\text{mfs}(G)}$ the *degradation* of the decomposition of P into G .

* Chargé de Recherches du FNRS.

** Research supported by NSF grants CCF-1018370, CCF-0430849 and by an Alfred P. Sloan fellowship. Research partially completed as a visiting professor at MADALGO (Center for Massive Data Algorithmics, a Center of the Danish National Research Foundation), Department of Computer Science, Aarhus University, IT Parken, Åbogade 34, DK-8200 Århus N, Denmark.

Minimum feature size effectively describes the global resolution needed to visually distinguish elements in a mesh. For example, it measures the maximum (uniform) thickness that the edges in a mesh can be drawn without obscuring the individual components. Also, mfs measures the (maximum) error allowed in the placement of vertices while still guaranteeing preservation of the topology of the mesh. We were originally motivated to study minimum feature size as a way to obtain pseudopolynomial bounds on algorithms (specifically, geometric dissection) that start with a triangulation step; see Section 5 for details.

One important issue is the type of desired triangulation, which we show has a significant effect on the results that can be achieved. Refer to Figure 1. The most common decomposition of a polygon is the *classic triangulation*, which adds noncrossing chords between pairs of vertices of P , until the interior of P is partitioned into triangles. A *nonproper triangulation* allows the addition of Steiner points (extra vertices), and noncrossing edges between pairs of vertices (original or added), until each interior face has the geometric shape of a triangle. A *proper triangulation* has the additional property that any two edges that lie on the same interior face and are incident to a common vertex are not collinear; in other words, each interior face consists of only three vertices.

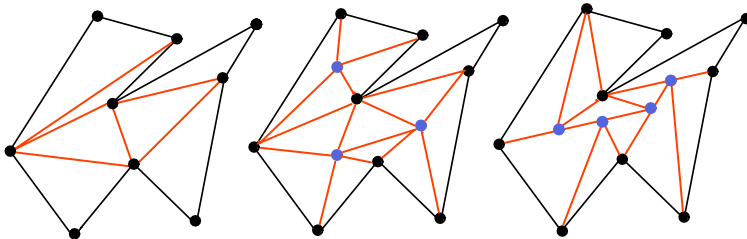


Fig. 1. Triangulation types: classic, proper, nonproper. Steiner points are blue.

Related results. Steiner points are necessary to obtain a degradation smaller than linear. Mitchell constructed two illustrative examples, described in [BDE95]. The first example is a regular n -gon: all classic triangulations have a degradation of $\Omega(n)$ (consider an ear). The second example is an $r \times 1$ rectangle with two additional vertices approximately midway along one long edge, spaced at unit distance from each other: all classic triangulations have a degradation of $\Omega(r)$. Here r is the ratio of the polygon’s diameter divided by its minimum feature size, often called the *spread*. These lower bounds extend to quadrangulations or any decomposition with constant-complexity faces; in the latter example, we simply add more vertices midway along the long edge.

When studying this problem, Bern, Dobkin, and Eppstein [BDE95] applied the notion of *internal feature size* $\text{ifs}(P)$, which is the minimum distance *inside* P between a vertex and a nonincident edge⁵. They proved that every polygon P (possibly with holes) has a proper triangulation G in which every triangle has height $\Omega(\text{ifs}(P))$, and thus $\text{ifs}(G) = \Omega(\text{ifs}(P))$. In other words, they achieve $\mathcal{O}(1)$ degradation for the interior

⁵ Note that “internal feature size” is called “minimum feature size” in [BDE95].

of P . However, this process can substantially reduce the minimum feature size (externally). Consequently, the first open problem the authors list is whether their result can be generalized to planar straight-line graphs.

In fact, Ruppert’s Delaunay mesh refinement algorithm had already claimed constant degradation for proper triangulation of planar straight-line graphs [Rup93, Theorem 1],⁶ but the “constant” actually depends on the minimum angle of the input graph (as well as the minimum triangle angle guaranteed by the algorithm).

Our results. We address the open problem of [BDE95] by showing that PSLGs have proper triangulations with $\mathcal{O}(\lg n)$ degradation. This is the first triangulation algorithm to achieve a reasonable bound on degradation; even for polygons, the only previous results bound internal feature size, not minimum feature size. Our algorithm uses $\mathcal{O}(n)$ Steiner points and hence $\mathcal{O}(n)$ triangles, and runs in $\mathcal{O}(n)$ time.

In [ADD⁺11], we argue that $\Omega(\lg n / \lg \lg n)$ degradation is in fact necessary for minimum feature size, even in polygons. This implies that our upper bound is nearly tight, and resolves the open problem mentioned above. This lower bound applies even to quadrangulation or any decomposition into constant-complexity faces. We are currently working on the details of improving this result to $\Omega(\log n)$, which would completely settle this question.

We also show a separation between proper and nonproper triangulations. Specifically, by allowing Steiner points along the sides of triangles, we show that PSLGs have nonproper triangulations with $\mathcal{O}(1)$ degradation, which is clearly optimal up to constant factors. We actually present this nonproper upper bound first, in Section 2, before describing the simple modifications needed to obtain $\mathcal{O}(\lg n)$ degradation for proper triangulations in Section 3. Our method can also be used to re-obtain the $\mathcal{O}(1)$ internal feature size degradation result of [BDE95]; see Section 4.

In all of our upper bounds, we focus on the case of triangulating a single polygon using small degradation. It is trivial to extend to polygons with holes. Because our triangulations do not add Steiner points to the boundary of the polygon, and because they approximately preserve minimum feature size instead of just internal feature size, they can be applied separately to each face of a PSLG to obtain the claimed results.

Table 1 summarizes the best results on degradation for each type of triangulation.

Type of triangulation	Degradation of	
	minimum feature size	internal feature size
Classic	$\Omega(n + r)$ [BDE95]	$\Omega(n + r)$ [BDE95]
Proper	$\Omega\left(\frac{\log n}{\log \log n}\right)$ [ADD ⁺ 11], $\mathcal{O}(\log n)$ [§3]	$\Theta(1)$ [BDE95] [§4]
Nonproper	$\Theta(1)$ [§2]	$\Theta(1)$

Table 1. Results on degradation, by triangulation type, when meshing a worst-case polygon or PSLG with n vertices and spread r .

⁶ Incidentally, this is also the paper that first introduced the notion of feature size.

2 Nonproper Triangulation

In this section, we show how to construct a nonproper triangulation of any polygon P with a degradation of $\Theta(1)$. We use $\Theta(n)$ Steiner points, and the construction can be computed in linear time.

We begin by explaining how to triangulate parallelograms and trapezoids. Trivially any rectangle can be triangulated by placing a Steiner vertex at its center. The mfs will degrade by a factor of 2. Suppose instead that we are given a parallelogram P with top and bottom edges horizontal, and tilted toward the right. A segment with one endpoint at the lower-right vertex determines $\text{mfs}(P)$. Its direction depends on the height of P and the length of the horizontal edges. The segment is either vertical representing the height, or orthogonal to the left edge of P . Either way, placing the Steiner vertex at the center yields a degradation of 2, as can be easily verified by examining similar parallelograms. Specifically the new mfs will be determined by a segment parallel to the original one, from the Steiner vertex to the boundary of P .

Lemma 1. *Any trapezoid H can be triangulated with a degradation $d_{\text{trap}} \leq 2$.*

Proof. Let L be the shorter of the parallel edges on H , with length ℓ , and without loss of generality, at the bottom of H . Let U be the top edge of H , and h be the height of H . Consider the rectangle R obtained by projecting L vertically upward onto the line through U . Suppose that R is contained in H . Then $\text{mfs}(H) = \min\{h, \ell\}$ (i.e., it is determined by the dimensions of R). We place a Steiner vertex s at the middle of R . The distance from s to L or U is $\frac{h}{2}$. The distance from s to the sides of H is greater than $\ell/2$. So if $h \leq \ell$, the degradation of the resulting triangulation is 2. Otherwise it is even less.

Now suppose that R is not contained in H , in which case we know that both side edges of H are slanted in the same direction, and without loss of generality, toward the right. Then $\text{mfs}(H)$ is determined by a segment with one endpoint on the lower-right vertex of H . Consider the parallelogram P obtained by sweeping a horizontal segment of length ℓ from L to U , while keeping its left endpoint on the left side of H . Then H and P have the same minimum feature size, determined by the same segment. The center of P is suitable for s . By construction, s separates P into four similar parallelograms. By preceding arguments described for parallelograms, the degradation of the resulting triangulation is 2. \square

Lemma 2 (Perturbation Lemma). *Moving all the vertices of a PSLG G by at most $\alpha \text{mfs}(G)$, for $\alpha < \frac{1}{2}$, results in a PSLG G' with degradation at most $\frac{1}{1-2\alpha}$ relative to G . The drawings of G and G' are combinatorially equivalent.*

Proof. Any distance determined by a point and a nonincident edge can be shortened by at most $\alpha \text{mfs}(G)$ at each end, and thus $2\alpha \text{mfs}(G)$ total. These distances were at least $\text{mfs}(G)$ to begin with. Combinatorial equivalence follows from the fact that no vertex is allowed to move enough to cross a nonincident edge. \square

The next lemma is essentially the most critical element of the main theorem that will follow.

Lemma 3. *Let R be a rectangle with $\text{mfs}(R) = w$ and height $h > w$. Let E be either the top or bottom edge of R , with length $c \cdot w$ for some integer c . Let Z be the set of positions on E , at distances $j \cdot w$ from one endpoint, for integers $0 \leq j \leq c$. If R has no Steiner vertices on its boundary, except possibly for positions in the set Z , then R can be nonproperly triangulated, without placing any additional Steiner vertices on its boundary, with constant degradation. Furthermore the number of additional Steiner vertices (inside R) is $O(c)$.*

Proof. The proof is by construction, specifically the triangulation G shown in Figure 2 (C), where as a worst-case scenario we have placed Steiner vertices at every multiple of w on the bottom edge of R .

The main construction has a set of edges anchored at one corner of R (upper-left in the figure). Starting from the shortest (and most clockwise), each such edge e_i reaches to a horizontal coordinate twice as large as the previous one, and to a vertical coordinate $\frac{h}{3}$ from the bottom, where it meets the midpoint of a vertical edge g_i of length $\frac{2h}{3}$. Also, between every two such successive edges g_i , there is a region below one of the anchored edges, that has a sawtooth pattern matching the Steiner vertices. Specifically, for e_i , the sawtooth region is bounded by e_i, g_i, g_{i-1} , and the bottom edge of R .

Among the newly constructed Steiner vertices on e_i (i.e., on the top side of its corresponding sawtooth), the leftmost, s_0 , is closest to edge e_{i+1} . This vertex happens to be the intersection of e_i with g_{i-1} . Because e_{i+1} reaches twice as far as e_i , but to the same vertical coordinate, the vertical separation between e_{i+1} and s_0 is $\frac{h}{6}$. The horizontal separation between e_{i+1} and s_0 is at least w . We conclude that the distance between e_{i+1} and s_0 is at least $w \frac{h}{6} \frac{1}{\sqrt{(\frac{h}{6})^2 + w^2}}$. This distance lower bounds the feature size of all triangles emanating from the top-left of R .

Each sawtooth consists of the bottom horizontal edge, two vertical edges (the left twice the length of the right), and a tilted top, where the tilt angle gets closer to horizontal as the sawtooths move further to the right. The minimum distance created within any sawtooth occurs at its right hand side and is determined by the angle of the internal diagonals and by the tilt of the top. The distance is minimized as the tilt of the top increases and as the diagonal becomes less vertical. So, the minimum distance overall is to be found at the leftmost sawtooth, in its rightmost component (triangle). See Figure 3. The new distance introduced is at least $\frac{h}{3} \frac{w}{2} \frac{1}{\sqrt{(\frac{h}{3})^2 + (\frac{w}{2})^2}}$. Notice that both terms calculated imply constant degradation. \square

Now we prove the main theorem of this section:

Theorem 1. *Every n -gon has a nonproper triangulation with constant degradation, using $O(n)$ Steiner vertices.*

Proof. Let P be an n -gon with minimum feature size 1. Let the curve P_2 be the locus of points inside P that have minimum distance $\frac{1}{4}$ from ∂P . This is obtained from the well-known grassfire transformation. P_2 is a closed curve consisting of n line segments (one per segment of P) as well as one circular arc corresponding to every reflex vertex of P . Each such arc spans less than 180° . See Figure 4 for an illustration of this process. Because P has minimum feature size 1, each line segment in P_2 has length at least $\frac{1}{2}$ (see Appendix A).

-
- (A) Classic triangulation of R with all 66 vertices on the bottom edge. Observe that the interiors of many of the triangles are not discernible.
- (B) Proper triangulation of R with all 66 vertices present, using a recursive construction. Here all triangles are discernible, but as the aspect ratio of R increases, the minimum feature size will slowly degrade.
- (C) Nonproper triangulation of R , using a novel construction. The triangulation is much easier to see than the previous two, and generalizing it to longer rectangles will not change the minimum feature size beyond that of this figure. The top figure shows the construction when all 66 vertices are present. The bottom figure illustrates how it can be adapted when vertices are not placed at all positions in Z .
- (D) This polygon illustrates that Steiner vertices cannot be placed on a significant fraction of the boundary close to the reflex vertex. A construction like one of the three above can be used to triangulate the gray shaded area.

Fig. 2. Triangulations of a long rectangle R , with the properties stated in Lemma 3. In this figure, R has a set Z of 66 evenly spaced positions on the bottom edge. Vertices occupy some (or all) positions in Z , and the triangulations do not add more vertices on the boundary. Also illustrated is an example of why the ability to triangulate R in such a way is important.

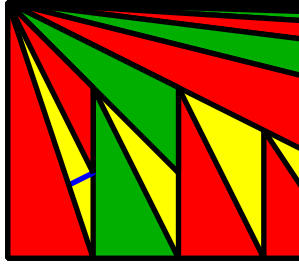


Fig. 3. Closeup of Figure 2 (C); a short blue edge highlights the distance that defines the minimum feature size for the construction of R in Lemma 3.

P_2 splits the interior of P into two regions, which we call the *Interior* and the *Tube*. P_2 itself belongs to both regions. We will modify and refine this boundary a few times, and then triangulate each region separately. Any operations in the interior of one region will not affect degradation in the other.

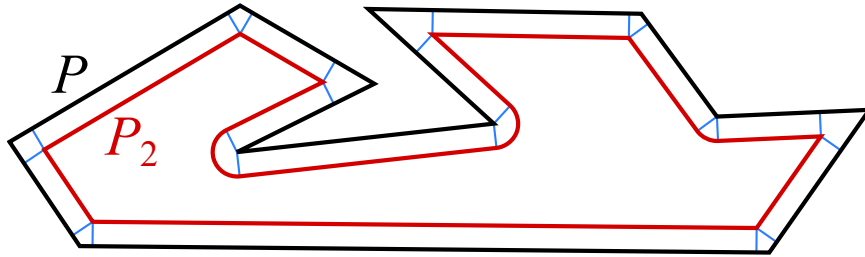


Fig. 4. A polygon P and the closed curve P_2 created by the grassfire transformation.

Refinement of P_2 : Refer to Fig. 5. We create a polygon P_3 by replacing all circular arcs on P_2 with polylines. Let O be a given circular arc with endpoints a_1 and a_2 . If O spans more than 90° , we can replace it with segments a_1m and ma_2 , where m is the midpoint of the arc. The minimum distance between P_3 and P is $\frac{1}{4\sqrt{2}}$ (achieved when O approaches 180°). So far, this distance lower bounds the feature size of the Tube, because (when $O = 90^\circ$) the segments on P_3 can have length as short as the side of a regular octagon of diameter $\frac{1}{4}$. That is, $\frac{1}{4}2 \sin \frac{\pi}{8} \approx 0.19$. We say that the Tube degradation is at most $d_{Tube3} = 4\sqrt{2}$. On the other hand, the feature size $\frac{1}{d_3}$ of the Interior is $\frac{1}{4}2 \sin \frac{\pi}{8}$, i.e., the feature size is smallest on its boundary P_3 . Distances through the interior of P_3 are still at least $\frac{1}{2}$.

If instead O spans less than 90° , we extend its adjacent edges on P_2 , through a_1 and a_2 respectively, until they meet. This extension remains at a distance greater than $\frac{1}{4}$ from P , so the Tube degradation is unaffected. The extension also remains at most $\frac{\sqrt{2}}{4}$ from the vertex on P that generated the arc (the max is achieved when the angle is 90°). All other points on P_3 are even closer to the boundary of P . Thus no two points from different edges on P_3 will get closer than $1 - \frac{\sqrt{2}}{2}$ to each other (roughly 0.29, not enough to reduce our bound on the feature size of the Interior).

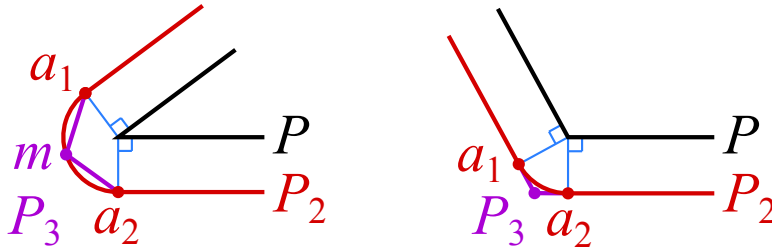


Fig. 5. How to transform P_2 to P_3 . Left: arc spans more than 90° ; Right: arc spans less than 90° .

Let P_4 be formed by snapping the vertices of P_3 vertically to a horizontal grid of granularity $g = \frac{1}{2d_3}$. Any point can snap at most a distance of $\frac{1}{4d_3}$; half the grid size. A pair of points on P_3 at a *nearly* co-vertical position a distance of $\frac{1}{d_3}$ from each other may snap toward each other, so snapping can degrade the feature size of P_3 , and thus also the Interior, by a factor of 2. The effect on the minimum distance between P and P_3 is smaller, because vertices of P remain fixed. This distance can drop to $\frac{1}{d_{tube3}} - \frac{1}{4d_3}$. At this point though, the minimum distance in both regions is to be found on their common boundary, and the value is $\frac{1}{2d_3}$.

Triangulation of Interior: Let P_5 consist of P_4 and the horizontal trapezoidation of the interior of P_4 . All vertices on P_4 lie on the grid and thus the feature size is preserved. Let P_6 consist of the triangulation of P_5 obtained by placing a vertex in each trapezoid according to the method presented in Lemma 1. Thus, the degradation in this step is $d_6 = d_{trap}$.

The total degradation of the Interior is therefore $2d_3d_6$. The feature size of the Interior is $\frac{1}{8} \sin \frac{\pi}{8} \approx 0.047$.

Triangulation of Tube: Obtaining a triangulation of the Tube is done without adding more Steiner vertices to its boundary, and thus any degradation in this process will not amplify the degradation of Interior, or affect feature size via the exterior of P .

Before proceeding to the algorithm, which has four main steps, we require one definition: A *quasi-trapz* is a quadrilateral that can be transformed into a trapezoid by perturbing its vertices by an amount small enough so that the Perturbation Lemma can be applied.

1. **Subdivision of the Tube into triangles and quasi-trapz.** Consider all convex polygonal chains that were created in P_3 as replacements of circular arcs spanning more than 90° on P_2 . Recall that such chains consist of two segments, which by now can also contain Steiner vertices from the trapezoidation of P_4 . For each chain, we connect the endpoints to the unique reflex vertex v_r of P that generated the corresponding (replaced) arc via the grassfire transform. Similarly, we connect every convex vertex of P to its corresponding convex vertex on P_4 , and we connect reflex vertices of P (with arcs spanning less than 90°) to their unique corresponding reflex vertex on P_4 . This subdivides the Tube into quasi-trapz and *convex fans* (i.e., a vertex visible from a convex chain). In fact any such fan is just a quadrilateral, because the chain opposite v_r had only two edges on P_3 (with Steiner vertices added later on). See Figure 6.

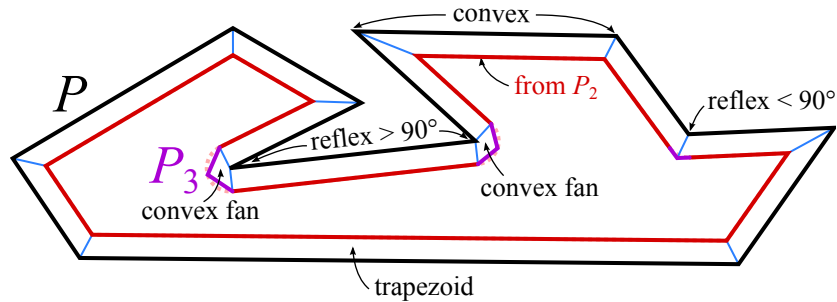


Fig. 6. Phase 1 of Tube triangulation: Subdividing Tube into fans and quasi-trapz. Angles indicated correspond to arc spans.

The only degradation caused can be due to a newly created edge, e , and some non-incident vertex p on P_4 . What matters is the angle that e makes with P_4 , and the proximity of p to the endpoint of e on P_4 . The latter is at least $\frac{1}{2d_3}$. Without taking snapping into account, the aforementioned angle would be no less than 45° . See Figure 7. So, adding these edges would only degrade feature size from $\frac{1}{2d_3}$ by a factor of $\sqrt{2}$. This means that the feature size of the fans could drop to roughly 0.067. This is not close to the smaller feature size in other areas that will be created, and snapping the vertices of the fan will not have any significant effect. The snapping would have to be so extreme that the angle mentioned would drop from 45° to under 14° . This is not possible when two vertices of a triangle move by less than a quarter of the shortest length.

We continue to triangulate each fan by adding diagonals from v_r to all remaining vertices within. The preceding analysis follows verbatim. Structurally, the end result is that any nontriangulated region of the Tube is a quasi-trapz that has an edge of P (the *bottom*) and an edge of P_4 (the *top*) on its boundary. Were it not for the snapping, the top and bottom would be parallel, and the quasi-trapz would be a trapezoid. Note that the top can contain Steiner vertices, generated during the trapezoidation of P_4 .

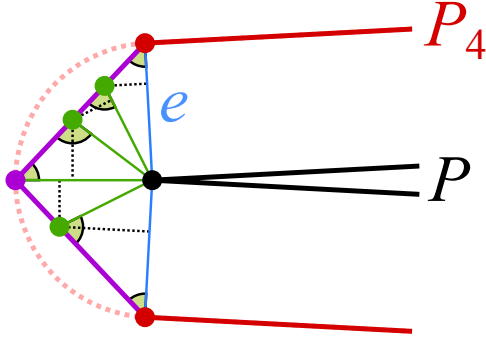


Fig. 7. Triangulating a convex fan: the angle between P_4 (purple) and edge e (blue) is at least 45° . The same holds for other edges (green) from P to Steiner points on the fan (which may have been introduced when constructing P_6 from P_4). Dotted black segments are minimum distances in newly created triangles.

- Subdivision of quasi-trapz with Steiner vertices on the top.** We will subdivide quasi-trapz so that the only remaining nontriangulated regions will be quasi-trapz without Steiner points on their boundary, and rectangles possibly with such Steiner points.

Let Q be a quasi-trapz to be subdivided. By assumption, Q has at least one Steiner vertex on its top, T . We will start adding diagonals from the bottom, B , to Steiner vertices on T . This will progressively cut off triangles, leaving a smaller quasi-trapz Q' . As we do this, we will be shortening T , so that it either has no Steiner vertices on it, or the internal angles of Q' at T are at least 135° . This will also imply that T comfortably projects onto the bottom, B , in a direction orthogonal to T .

For each endpoint t of T with internal angle smaller than 135° (note that the angle is at least 45° to start with), do the following. Let v be the neighbor of t on Q , on edge B . Traverse T from t until a Steiner vertex s is found, and join s to v . While the angle condition is not met, keep forming such an edge to v for each successive s . This repeatedly cuts off triangles from Q , until it is either a triangle or Steiner-free quasi-trapz (if no more Steiner vertices remain), or until the angle condition is satisfied. The triangles cut off on each side form a convex fan triangulation (with v as the apex), identical in nature to those described in phase 1. Thus the degradation caused so far can be absorbed into the preceding analysis. See Figure 8.

Let T' be the subset of T left over from this process (see Figure 8). Now T' and B form the parallel edges of Q' , which is a subset of Q . Consider the shape of Q' as it existed before snapping. Recall that before snapping, T' and B were parallel, at distance $\frac{1}{4}$. The minimum feature size of Q' is lower bounded by the separation of Steiner vertices on its boundary, i.e., $\frac{1}{2d_3}$. Let a and b be the endpoints of T' . Let a' and b' be vertices placed at a distance $\frac{1}{4} - \frac{1}{2d_3}$ away from a and b , respectively, so that $baa'b'$ is a rectangle R inside Q' . Notice that a' and b' are $\frac{1}{2d_3}$ from B , and even further from the sides of Q' . So this placement doesn't affect the feature size. Now, connect a' and b' to the vertices on Q' . Inside Q' , we are left with a Steiner-

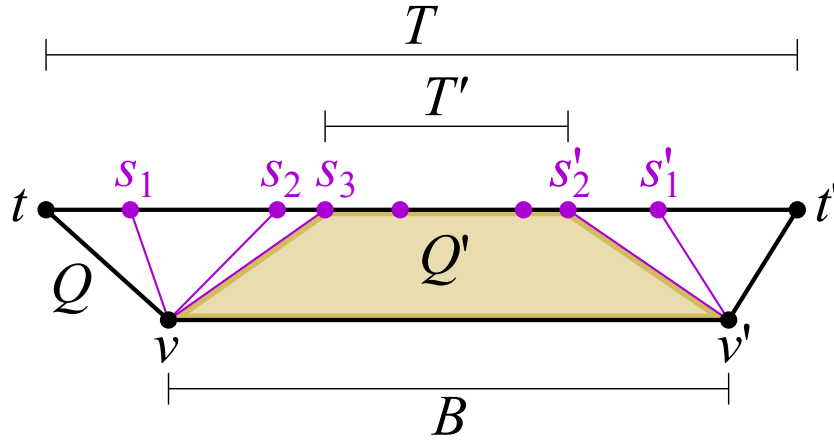


Fig. 8. Phase 2 of Tube triangulation: decomposing Q into Q' and triangulated fans. Either the internal angles of Q' at the top are greater than 135° , or Q' has no Steiner vertices.

free trapezoid Q'' (it is below $a'b'$ and will again become a quasi-trapz when we account for snapping), the rectangle R with Steiner points on the edge ab , and two triangles. See Figure 9.

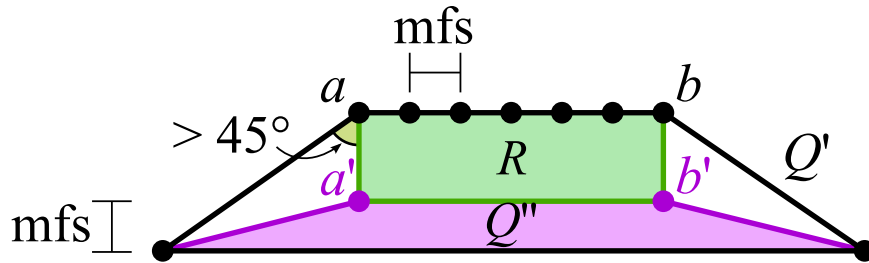


Fig. 9. Phase 2 of Tube triangulation: decomposing Q' into R and Q'' .

Finally we must reinstate the snapping of the segment ab . The positions of a' and b' will follow so that R moves rigidly. We now examine the effect of the motion of a' on the feature size of the components of Q' . Recall that a' is snapped by at most $\frac{1}{4d_3} = \frac{1}{16\sqrt{2}}$ (roughly 0.044). So it can reduce the feature size of Q'' to $\frac{1}{4d_3}$ (by moving half way to the fixed edge B on Q''). The effect of a' is even smaller on the feature size of the triangles in Q' , because its distance to their nonincident edges is greater than its distance to B . Of course, there is no effect on R .

3. **Triangulate all remaining Steiner free quasi-trapz.** Here we triangulate any quasi-trapz Q'' constructed in the previous phase. One Steiner vertex s suffices, as with any trapezoid. There is a placement for s in the corresponding unsnapped trapezoid Q so that degradation is no more than 2. Because Q has height $(\frac{1}{2d_3})$, s

would normally be placed between the parallel edges of Q , i.e., $\frac{1}{4d_3}$ from B . However the edge $a'b'$ might snap by this much, and this would create an arbitrarily small distance to s . So, instead we will place s at a distance $\frac{1}{8d_3}$ from B , because B will remain fixed. The effect is that the feature size of Q'' can be reduced to $\frac{1}{8d_3}$, but no less. Currently, this quantity lower bounds the overall feature size, at roughly 0.022. See Figure 10.

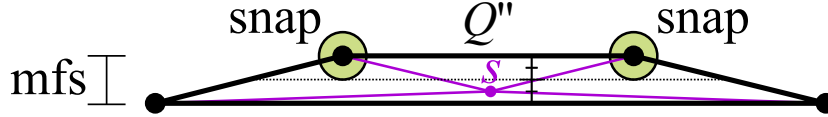


Fig. 10. Phase 3 of Tube triangulation: handling the last remaining quasi-trapz.

4. **Triangulate rectangles generated in phase 2.** For each rectangle $R = abb'a'$, we use the construction presented in Lemma 3. R has height $h = \frac{1}{4} - \frac{1}{2d_3}$, and Steiner vertices are placed on one of its longer sides, at distances of $\frac{1}{2d_3}$. Then the formula in Lemma 3 yields a value of greater than 0.024 for $\text{mfs}(R)$.

The important conclusion is that each step described incurs a constant degradation, therefore the aggregate is also constant. Most of the steps described probably have tighter bounds. Furthermore, these steps could be optimized to work more harmonically, or replaced with more efficient constructions. For the record, we claim here that the degradation is under 45 (the inverse of 0.022 calculated in phase 3 in the Tube).

The construction of P_3 adds a linear number of Steiner vertices, since a constant number of them is associated with each vertex of P . No Steiner vertices are added when we form P_4 , since this only involves snapping. P_5 is a trapezoidation formed by extending a line from every vertex. This creates a linear number of Steiner vertices (and trapezoids). As we construct P_6 , we add one Steiner vertex per trapezoid. Thus the boundary and interior of P_2 contain a linear number of Steiner vertices. Finally, when we triangulate the Tube, we only add Steiner vertices to the interior. Step 1 adds no vertices. Step 2 adds two vertices to form Q'' and R , in each quasi-trapz. Step 3 adds one vertex per quasi-trapz. There is one quasi-trapz per edge of P , so all of these steps add a linear number of Steiner vertices. Step 4 adds a number of vertices proportional to the number of vertices on the boundary of the rectangle R (by Lemma 3). The total number of vertices on all such rectangle boundaries is $O(n)$, because they are formed when processing the interior of P_2 . \square

3 Proper Triangulations

Next we describe the few modifications necessary for proper triangulations, which lose a logarithmic factor in minimum feature size:

Theorem 2. *Every n -vertex polygon has a proper triangulation with $O(\log n)$ degradation.*

Proof. Use the algorithm of Section 2, with the exception of the nonproper triangulation of the rectangle $R = abb'a'$. That triangulation is instead done using the construction of Figure 2 (B). This is a simple recursive decomposition of a rectangle into proper triangles. For n vertices on the bottom of R , there are $O(\log n)$ horizontal layers in the construction. The separation between those vertices defines the minimum feature size of the input. The height of R could also equal this value (any more only helps to preserve feature size). Therefore the construction of these layers can cause a degradation of $O(\log n)$. Triangulating the layers only affects the multiplicative constant. \square

4 Internal Feature Size

For internal feature size in a polygon, we can avoid losing constant degradation or properness. This result is already known [BDE95], but can also be obtained by our methods:

Theorem 3. *Every n -vertex polygon has a proper triangulation with $O(1)$ internal feature size degradation.*

Proof. The only component where our triangulation from Section 2 is nonproper is within the quasi-trapz in the Tube, or more specifically, the rectangular regions. Instead, if we are not concerned with external feature size, we can triangulate the quasi-trapz by creating Steiner vertices on the boundary of P , to match those on the inner boundary of the Tube. \square

5 Pseudopolynomial Dissection

Our original motivation for finding meshes that approximately preserve minimum feature size came from the classic problem of *geometric dissection*. The nearly 200-year-old algorithm of Lowry [Low14, Fre97] *dissects* any two given polygons P^1, P^2 of equal area into polygonal pieces such that the pieces of P^1 can be translated and rotated to make up the pieces of P^2 . Unfortunately, the number of pieces it uses can be extremely large.

How many pieces does polygon dissection need? In particular, do a pseudopolynomial number of pieces suffice? In computational geometry, a *pseudopolynomial* bound is polynomial in the number n of input coordinates and the size of a grid needed to express those coordinates. The latter bound is typically approximated by the *spread* $r = D/w$, where D is the diameter and w is the minimum feature size.⁷ Some dependence beyond n is necessary for dissection: for example, dissecting a square into an $r \times 1$ rectangle requires $\Omega(\sqrt{r})$ pieces by a simple diameter argument.

We prove here that any two polygons P^1 and P^2 have a dissection using $(n(P^1) + n(P^2)) \cdot (r(P^1) + r(P^2))$ pieces. This result follows by combining Lowry’s original algorithm with an ifs-preserving triangulation algorithm, such as ours or the one in [BDE95]. More generally, for k polygons P^1, \dots, P^k , we obtain a dissection using $k(n(P^1) + \dots + n(P^k)) \cdot (r(P^1) + \dots + r(P^k))$ pieces.

⁷ This parameter also arises in many meshing results; we saw one in Table 1.

Lowry’s algorithm starts by triangulating the polygon P^1 , and then uses a dissection of Montucla from 1778 (see [Fre97]) to convert each triangle into a rectangle with a common height ε . The largest suitable ε is half the minimum height of all triangles, i.e., half the internal feature size of the triangulation. The common-height rectangles can then be assembled into one $A/\varepsilon \times \varepsilon$ rectangle, where A is the area of P^1 . The resulting number of pieces is $\mathcal{O}(nA/\varepsilon)$; furthermore, each piece is bounded by a constant number of cuts, and the number of cuts hit by any vertical line is $\mathcal{O}(1)$. Finally the algorithm repeats this process for P^2 , and overlays the two dissections of the $A/\varepsilon \times \varepsilon$ rectangle. By the properties above, this overlay increases the number of cuts and thus pieces by only a constant factor, resulting in $\mathcal{O}((n(P^1) + n(P^2))A/\varepsilon)$ pieces. More generally, for k polygons, each cut can be divided k times, so we obtain a piece bound of $\mathcal{O}(k(n(P^1) + \dots + n(P^k))A/\varepsilon)$.

Lowry’s algorithm does not specify a triangulation, so cannot efficiently bound ε . While a classic triangulation was originally intended, any nonproper triangulation suffices. Using an ifs-preserving triangulation, we obtain a triangulation with $\varepsilon = \Theta(\text{ifs}(P^1))$. Rescaling to make $A = 1$ does not affect the algorithm, and uses a scale factor no smaller than $\mathcal{O}(1/D)$, where D is the diameter of any polygon. Thus we obtain $\varepsilon = \Omega(\text{ifs}(P^1)/D) = \Omega(1/r)$ and $A = 1$. Plugging these bounds into the piece bound above, we obtain the desired result.

6 Discussion

Although several steps in our construction require subtle constructions and details to keep things at constant distance, we believe that the essential hurdle was how to triangulate rectangles with many Steiner points on a side, without adding new Steiner points on the boundary. This was the breakthrough needed to solve the problem at hand.

Preserving minimum feature size is by no means the only priority in meshing, but it is still a meaningful (and well-studied) measure of mesh quality. We leave to future work the possibility of simultaneously attaining small feature-size degradation with other important mesh properties, such as maximum angle bounded away from 180° . This goal may be attainable by simply combining algorithms in a careful way.

Another direction for further research would be to extend our results to 3D. Our grassfire approach should work just as well. The central challenge, as in 2D, would seem to be the proper triangulation (tetrahedralization) of a box that is very thin in one or two of its dimensions.

Acknowledgments

This research was initiated at the 24th Annual Winter Workshop on Computational Geometry, co-organized by Erik Demaine and Godfried Toussaint, and held at the Bellairs Research Institute of McGill University in February 2009. We thank the other participants of the workshop for their helpful comments and for creating an environment conducive to creative thought: Zachary Abel, Brad Ballinger, Nadia Benbernou, Prosenjit Bose, Jean Cardinal, Sébastien Collette, Mirela Damian, Robin Flatland, Ferran Hurtado, Scott Kominers, Stefan Langerman, Robbie Schweller, David Wood, and Stefanie Wuhrer.

References

- ADD⁺11. Greg Aloupis, Erik Demaine, Martin Demaine, Vida Dujmovic, and John Iacono. Meshes preserving minimum feature size. Technical report arXiv:0908:2493, 2011.
- BDE95. Marshall Bern, David Dobkin, and David Eppstein. Triangulating polygons without large angles. *Interational Journal of Computational Geometry & Applications*, 5(1–2):171–192, March–June 1995.
- BE95. Marshall Bern and David Eppstein. Mesh generation and optimal triangulation. In Ding-Zhu Du and Frank Kwang-Ming Hwang, editors, *Computing in Euclidean Geometry*, number 4 in Lecture Notes Series on Computing, pages 47–123. World Scientific, second edition, 1995.
- Dey07. Tamal K. Dey. Delaunay mesh generation of three dimensional domains. Technical Report OSU-CISRC-09/07-TR64, Ohio State University, October 2007.
- Eri03. Jeff Erickson. Nice point sets can have nasty delaunay triangulations. *Discrete & Computational Geometry*, 30(1), July 2003.
- Fre97. Greg N. Frederickson. *Dissections: Plane and Fancy*. Cambridge University Press, November 1997.
- HMP06. Benoit Hudson, Gary Miller, and Todd Phillips. Sparse Voronoi Refinement. In *Proceedings of the 15th International Meshing Roundtable*, pages 339–356, Birmingham, Alabama, September 2006. Springer-Verlag.
- Low14. Mr. Lowry. Solution to question 269, [proposed] by Mr. W. Wallace. In T. Leybourn, editor, *Mathematical Repository*, volume 3, part 1, pages 44–46. W. Glendinning, London, 1814.
- Rup93. Jim Ruppert. A new and simple algorithm for quality 2-dimensional mesh generation. In *Proceedings of the 4th Annual ACM-SIAM Symposium on Discrete Algorithms*, pages 83–92, Austin, Texas, 1993.
- She04. Jonathan Richard Shewchuk. Theoretically guaranteed Delaunay mesh generation—in practice. Short course at 13th International Meshing Roundtable, 2004. <http://www.cs.berkeley.edu/~jrs/papers/imrtalk.pdf>.

A Offset Edge Lengths

Claim: Let C be the curve that is the locus of points inside polygon P , at distance $\frac{1}{4}$ from the boundary of P . If $\text{mfs}(P) = 1$ then every straight edge of C has length at least $\frac{1}{2}$.

C is obtained from P using the grassfire transform, commonly used as a visualization of the construction of the medial axis. Note that each edge e on P transforms to an edge e' on C continuously as the grassfire progresses. The shape of e' depends on local conditions; specifically the angles of vertices at the endpoints of e . Let e be positioned horizontally, between vertices p_1, p_2 . Suppose that the interior of P is below e . The edge e' must reside on the horizontal line at a distance $\frac{1}{4}$ below e .

If both endpoints of e are reflex vertices on P , then e' will have the same length. If one of the vertices is reflex (without loss of generality, the left, p_1), then the left endpoint v_1 of e' will be located vertically below p_1 , at a distance of $\frac{1}{4}$. Note that e' is just a subset of a longer edge on C . Follow a ray to the right of v_1 for a distance of $\frac{1}{2}$, to construct a point, x . Let J_{p_1} be the unit quarter-circle in the lower-right quadrant of p_1 . Then x is inside J_{p_1} and at a distance greater than $\frac{1}{4}$ from the arc of J_{p_1} . Thus x cannot be a vertex on C , because it is not at a distance $\frac{1}{4}$ from any point on P (excluding e itself). This implies that e' has length greater than $\frac{1}{2}$.

Finally, there is the case where both endpoints of e are convex vertices. Note that e' can have a length of $\frac{1}{2}$ if e has length 1 and both convex angles are 90° . Then, the endpoints of e' are directed inward at angles of 45° , relative to the endpoints of e . If $|e| = 1$, then both convex angles must be at least 90° , so $|e'| \geq \frac{1}{2}$.

We can make e larger to allow for smaller convex angles at its endpoints. If we do so, the worst scenario is one where the edges adjacent to e in P are angled in a way that they eventually have a distance of 1 with each other (i.e., we close the angles as much as possible without violating feature size of P). So, without loss of generality, assume that the angle at p_1 is less than 90° . Follow the edge u neighboring e to the left until hitting a horizontal line at a distance of 1 from e . Note that this intersection point, y , must exist, otherwise we contradict the mfs assumption about P (the endpoint of u would be too close to e). In other words y belongs to u . Construct the point z at a distance 1 vertically above y . This must be part of e , by construction. No part of the boundary of P intersects the triangle yzp_1 . The left endpoint t_1 of e' cannot be more than $\frac{1}{4}$ to the right of the segment yz ; this happens if the angle at p_1 is 90° , and as this angle decreases t_1 moves to the left relative to yz . To visualize this, it is convenient to consider yz fixed, and move p_1 to the left.

Consider the unit quarter-circle J_y centered at y , in its top-right quadrant. No part of P can intersect J_y ; if an edge not adjacent to y does so, it will be too close to y , and if an adjacent edge does so (if y were a real vertex), it will be too close to e . Now consider the vertex p_2 , common to e and its edge e_r to the right. Wherever p_2 is, $|e'|$ will be minimized if we minimize the angle at p_2 . If this angle is less than 90° , then because e_r must miss J_y , we follow the same reasoning as above to easily conclude that e' has length greater than 1. That is, the right end t_2 of e' will not be more than $\frac{1}{4}$ to the left of some vertical segment $y'z'$ analogous to yz .

So we are left with the case where p_2 has angle greater than 90° and is located within one unit of z , i.e., its vertical projection intersects J_y . As mentioned, $|e'|$ will be minimized if the angle at p_2 is minimized, which is to say that e_r should be rotated as clockwise as possible, until it becomes tangent to J_y . This means that the bisector at p_2 intersects y . So p_2 should be placed as close to z as possible, to minimize $|e'|$. We will now work within the triangle p_1yp_2 .

Let q be the intersection of yz with the line through e' . We know that t_2 will be to the right of q . On the other hand, t_1 can be arbitrarily to the left, or slightly to the right (specifically no more than $\frac{1}{4}$). Let $t_2 - z$ be e'_2 , and $z - t_1$ be e'_1 . Then $|e'|$ is equal to $e'_1 + e'_2$.

There is another constraint on the location of p_2 : it cannot be too close to u . Let ω be the angle at p_1 . Then $\sin \omega = \frac{1}{|e'|}$, meaning p_2 is placed so that its distance to u is 1. Let $z - p_1$ be e_1 . From triangle yzp_1 we have $\tan \omega = \frac{1}{e_1}$.

Let e_2 be $p_2 - z$. Triangle yzp_2 is similar to triangle yqt_2 , so $e'_2 = \frac{3e_2}{4}$. From the triangle formed by p_1 , t_1 , and the projection of t_1 onto e , we have $\tan \frac{\omega}{2} = \frac{0.25}{e_1 - e'_1}$; (t_1 is $\frac{1}{4}$ below e , and on the bisector of ω).

Reordering and combining from above, we have:

$$e'_1 = e_1 - \frac{1}{4 \tan \frac{\omega}{2}} = \frac{1}{\tan \omega} - \frac{1}{4 \tan \frac{\omega}{2}}. \text{ Because } e_2 = \frac{1}{\sin \omega} - e_1, \text{ we have}$$

$$e'_2 = \frac{3}{4} \left(\frac{1}{\sin \omega} - e_1 \right) = \frac{3}{4} \left(\frac{1}{\sin \omega} - \frac{1}{\tan \omega} \right).$$

Notice that when ω increases to 90° (i.e., p_1 approaches z from the left), we have $e'_1 = -\frac{1}{4}$ and $e'_2 = \frac{3}{4}$, so $|e'| = \frac{1}{2}$. For $\omega \leq 90^\circ$, e' is longer.